

# Estimating Fetal Nuchal Translucency Parameters from its Ultrasound Image

Yin-Hui DENG, Yuan-Yuan WANG  
Department of Electronic Engineering  
Fudan University  
Shanghai, China  
Email: yywang@fudan.edu.cn

Ping CHEN  
Ultrasound Department  
The First Maternity and Infant Health Hospital  
Shanghai, China

**Abstract**— Parameters of the fetal nuchal translucency (NT) are very important for the diagnosis and evaluation of fetuses. Currently these parameters are manually measured from the fetal ultrasound image, which may introduce problems of the variability and reproducibility. Here an automatic scheme is proposed to estimate fetal NT parameters. With a morphologic filtering, this scheme firstly establishes the edge map and extracts a preliminary contour by the gradient vector flow (GVF) snake. Then an algorithm based on the dynamic programming is proposed to compound the edge map and the preliminary contour to obtain the NT contour. Finally, parameters of the NT such as the NT thickness and the NT area are calculated. From the application, it is seen that this scheme simultaneously overcomes problems of discontinuousness and concavities in the contour extraction and parameters of the fetal NT can be automatically calculated.

**Keywords**—nuchal translucency; contour extract; morphologic filter; gradient vector flow; dynamic programming

## 1. INTRODUCTION

Ultrasound imaging is widely used in the diagnosis and evaluation of fetuses because of its noninvasive nature, its low cost, and continuing improvements in the image quality. Accumulation of fluid in the nuchal region, the nuchal translucency (NT), can be shown in the ultrasound image for all fetuses during the first trimester [1]. At 10-14 weeks of the gestation, a high proportion of fetuses with trisomies 13, 18 and 21 as well as Turner's syndrome and triploidies have ultrasonographically detectable NT thickness of at least 3 mm [2]. Even in the presence of a normal karyotype, a bigger NT thickness is also associated with structural defects and genetic syndromes [3]. NT thickness in the first trimester of pregnancy has proved to be one of the most discriminating parameters [4].

The NT thickness is measured in the sagittal section of fetuses by the transabdominal or transvaginal ultrasonography. Nowadays the measurement of the NT thickness is usually carried out by doctors. This requires highly skilled operators and leads to the variability of detected data. There is just a little study on an automated computerized measurement of the fetal NT. Bernardino *et al.* proposed a semiautomated computerized measurement scheme, which used the Sobel operator to detect the border of the NT [5]. It is also noted that the NT thickness is not completely related to some diseases [2]. Therefore, it is necessary to extract the NT's contour for further studies.

The NT contour in an ultrasound image often manifests a spindly section with a high intensity of discontinuousness.

National Basic Research Program of China (No. 2005CB724303), Natural Science Foundation of China (No.30570488) and Shanghai Leading Academic Discipline Project (No.B112).

Conventional contour extraction approaches don't fit this situation. There are two key difficulties. One is that the discontinuous intensity of the true contour often leads to the leakage of border [6]. The other is that active contours have difficulties to progress into boundary concavities [7], [8]. By defining proper internal forces and external forces, these difficulties can be well figured out respectively [6], [9]. However, in the NT measurement, these two key difficulties exist at the same time. Due to the antinomy of internal forces and external forces, there is no approach which can well solve two difficulties simultaneously.

In this paper, a novel scheme is proposed to extract the NT contour automatically. Firstly, ultrasound images are denoised by a morphological filter. Secondly, two points are set artificially in images to define the region of interest. Thirdly, a threshold process and the gradient vector flow (GVF) snake [9] are respectively used to collect the necessary image information. Finally, the NT contour is extracted by compounding the collected image information with an algorithm based on the dynamic programming [10]. After the NT contour is extracted, parameters of the NT such as the NT thickness and the NT area are calculated.

## 2. THE PROPOSED SCHEME

The proposed scheme is to overcome two key difficulties of the contour extraction mentioned above. With this scheme, the NT contour can be extracted from ultrasound images.

### 2.1. The Morphologic Filter

In ultrasound images, the speckle is the main noise which reduces the contrast and obscures diagnostically important details. From the viewpoint of visualization, the speckle appears in the image as narrow walls and valleys [11].

The basic method of morphologic filters [12] for despeckling is that it tears down the narrow walls (bright edges) and fills up the narrow valleys (dark edges) [13], [14].

The morphology defines gray scale dilation as an operation that selects the maximum pixel value from the mask window. Similarly, gray scale erosion is defined as an operation that selects the smallest pixel value from the mask window [12].

Gray scale dilation of  $f$  by  $b$ : denoted  $f \oplus b$ , is defined as

$$(f \oplus b)(s, t) = \max \{ f(s - x, t - y) + b(x, y) \mid (s - x, t - y) \in D_f; (x, y) \in D_b \} \quad (1)$$

Gray scale erosion of  $f$  by  $b$ : denoted  $f \ominus b$ , is defined as

$$(f \ominus b)(s, t) = \min \{ f(s + x, t + y) - b(x, y) \mid (s + x, t + y) \in D_f; (x, y) \in D_b \} \quad (2)$$

where  $D_f$  and  $D_b$  are domains of  $f$  and  $b$  respectively,  $s, t, x$  and  $y$  are coordinate indexes.

Morphological opening is defined as

$$f \circ b = (f \ominus b) \oplus b \quad (3)$$

Morphological closing is defined as

$$f \bullet b = (f \oplus b) \ominus b \quad (4)$$

Considering the NT size in ultrasound images, three small mask windows shown in Fig.1 are used for the horizontal, vertical, and diagonal morphological filtering. A morphological opening and a morphological closing are performed successively to an ultrasound image.

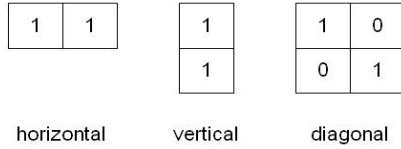


Figure 1. Three mask windows in the morphologic filter.

## 2.2. Selecting the region of interest

Because the NT is a very small section in ultrasound images, it is required to define a region of interest (ROI) to reduce the interference of other object boundary. The NT manifests a spindly section. In the proposed scheme, two endpoints of long axis inside the NT contour are labeled artificially. The process need not be exact to some extent. For a real fetal ultrasound image as shown in Fig.2(a), a simple polygon is constructed as the NT's initial contour with two endpoints shown in Fig.2(b).

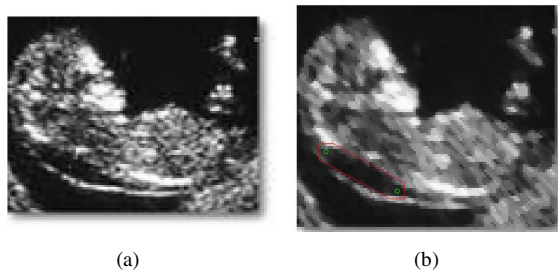


Figure 2. The NT's initial contour (b) for a fetal ultrasound image (a).

## 2.3. Collecting the necessary image information

Before extracting the NT contour, some necessary image information is needed.

### 2.3.1. The threshold process

A threshold process to obtain a binary image is applied as a preliminary process. In ultrasound images, the NT contour manifests a spindly section with a high intensity of

discontinuousness. The intensity of two initial points mentioned above represents the intensity of inside pixels of the NT contour.

Usually the NT contour's intensity is much larger than the intensity inside (and outside) the NT contour. A threshold value  $T$  is set as the mean intensity of two initial points plus an empirical parameter  $\alpha$ . Then the threshold process is applied to ultrasound images according to

$$f'(i, j) = \begin{cases} 0 & \text{if } f(i, j) > T \\ 1 & \text{if } f(i, j) \leq T \end{cases} \quad (5)$$

where  $f$  represents the ultrasound image,  $f'$  represents the image after the threshold process,  $i$  and  $j$  are coordinate indexes.

The contour information in the binary image after the threshold process is much clearer for the contour extraction. So the edge map is established from the binary image. It is noted that the intensity discontinuousness of the NT contour still remains, which should be coped with for the contour extraction.

### 2.3.2. The GVF Snake

For the contour extraction, the GVF field is a new external force model for active contours and deformable surfaces [9]. The field is calculated as a diffusion of gradient vectors of a gray or binary edge map. It allows for the flexible initialization of the snake or deformable surface and encourages the convergence to boundary concavities to some extent.

The NT's initial contour mentioned above is used as the initial curve of GVF snake. Then a GVF contour is obtained by the snake and the edge map established above. This contour is a close curve, which may not converge to boundary concavities very well.

### 2.4. Extracting the NT contour

From the GVF contour and the edge map, the final NT contour is extracted based on the dynamic programming.

Firstly, pixels in an ultrasound image are divided into four classes as shown in Table 1.

TABLE I. THE CLASSIFICATION CRITERION

class	The property of pixels	
	In the GVF contour	In the edge map
Class 1	Yes	Yes
Class 2	No	Yes
Class 3	Yes	No
Class 4	No	No

Pixels of class 1 are surely ones of the true NT contour. Pixels of class 4 are certainly not ones of the true NT contour. The GVF contour may not converge to boundary concavities well. So pixels of class 2 are more possible to be ones of the true NT contour than pixels of class 3.

The algorithm to extract the final NT contour is described as follows:

1. Record pixels of class 1 in the sub M.

2. With the GVF contour, deasil classify pixels of class 1 into  $k$  subclasses  $\{N_1, N_2, \dots, N_k\}$  according to their connectivity. Record two endpoints of each subclasses as  $\{[p_{11}, p_{12}], [p_{21}, p_{22}], \dots, [p_{k1}, p_{k2}]\}$ .

3. Establish an ordered pair sub as  $\{[p_{12}, p_{21}], [p_{22}, p_{31}], \dots, [p_{(k-1)2}, p_{k1}], [p_{k2}, p_{11}]\}$ . Assign pixels of class 1, class 2, class 3 and class 4 the cost value  $C_1, C_2, C_3$  and  $C_4$  respectively. Make sure  $C_1 > C_3 > C_2$ . So a cost map is built up.

4. For each ordered pair  $[p_{i2}, p_{j1}]$ , find the optimum path from  $p_{i2}$  to  $p_{j1}$  with the cost map based on the dynamic programming. Record pixels of each path in the sub M.

Assigning pixels of class 1 the largest cost value guarantees the direction and convergence of the dynamic programming. Two key difficulties mentioned above are figured out with this algorithm, which will be discussed in section 4.

Pixels in the sub M consist of the NT contour. With the NT contour, the NT thickness and NT area can be calculated.

### 3. EXPERIMENTAL RESULTS

#### 3.1. Experimental results

To illustrate the performance of the proposed scheme, we test it using both simulated and real B-mode ultrasound images.

Fig.3 shows the performance of the proposed scheme for a simulated image. Fig.3(a) is the simulated image and the pink curve is the contour needed to be extracted. In Fig.3(b) the green rectangle is the initial contour, the blue ring curve is the contour extracted by the GVF snake and the red curve is the final result of the proposed scheme.

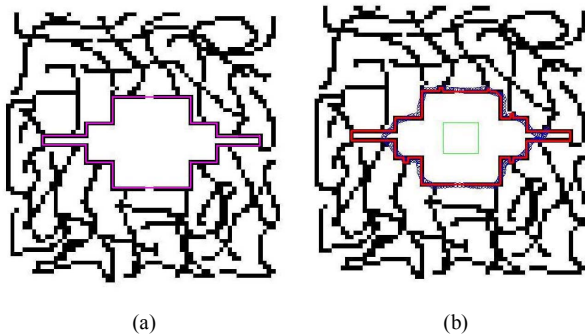


Figure 3. The result of the proposed scheme (b) for a simulated image (a).

It is seen that the proposed scheme can extract the expected contour very well.

For a real B-mode ultrasound image as shown in Fig.2(a), Fig.4 displays the morphologic filtered result compared with results of the speckle reducing anisotropic diffusion (SRAD) [15] under 20, 40 and 60 iterations respectively. The right column is the result of the threshold process for the left one accordingly.

It is seen that the morphologic filtered result outperforms the SRAD which is considered to be a competitive approach.

With the ROI as shown in Fig.2(b) and the edge map based on Fig.4(b), the GVF is established as shown in Fig.5(a) and the extracted GVF contour is shown in Fig.5(b).

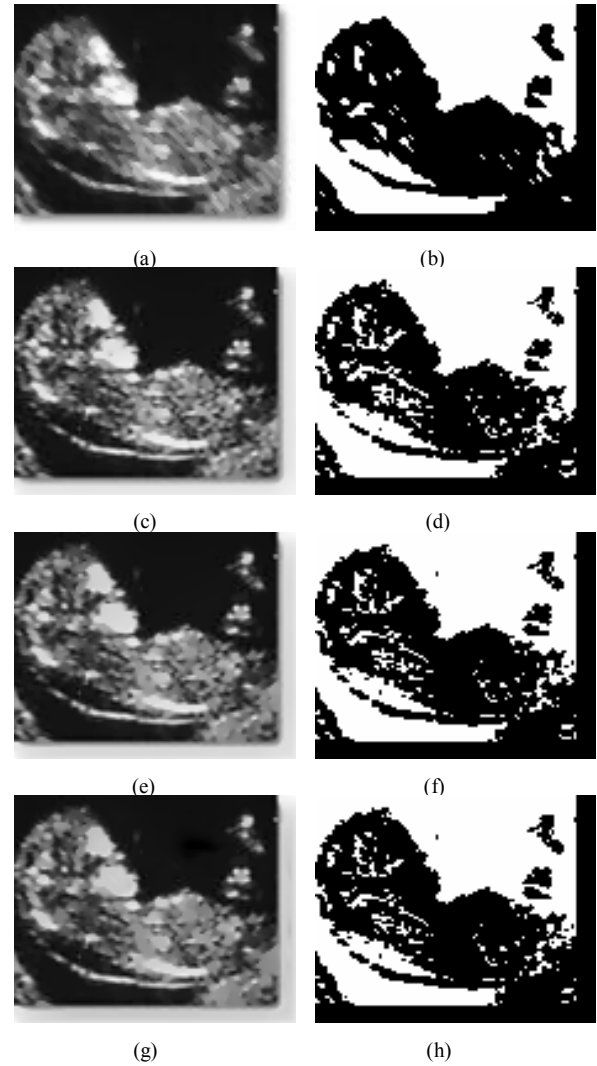


Figure 4. The comparison of filtered results, the first row is the result of the morphologic filter and the other rows are results of the SRAD under 20, 40 and 60 iterations respectively.

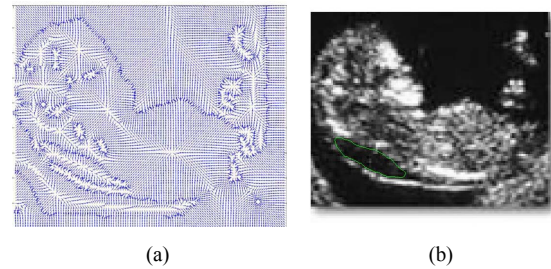


Figure 5. The GVF (a) and the GVF contour (shown in green) (b).

Fig.6 shows the result of the proposed scheme which demonstrates the exact and clear NT contour.

The experimental results of both simulated and real B-mode ultrasound images demonstrate the good performance of the proposed scheme, which simultaneously figures out two key difficulties of the contour extraction mentioned above.

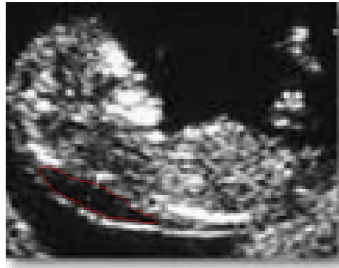


Figure 6. The result of the final NT contour (shown in red).

### 3.2. Parameter calculation

The NT contour can be well extracted from the ultrasound image with the proposed scheme. This makes the parameter calculations possible and easy.

The number of the pixels inside the NT contour is counted and represents the NT area. For the NT thickness, we firstly find two points on the contour which have the most Euclidean distance. A line is obtained by connecting these two points. Then an ordered pair on the NT contour with the most Euclidean distance is found along the orthogonal direction of the line. The length of the line by connecting the ordered pair represents the NT thickness.

## 4. DISCUSSION

### 4.1. The algorithm in the proposed scheme

The basic idea of the proposed scheme is that the contour extracted by the GVF snake is only regarded as the fundamental contour. Then pixels of the real contour are searched. If there is a closer curve in the edge map between two pixels on the GVF contour, this segmental GVF contour is replaced by the closer curve in the edge map. This is because pixels in the edge map are more possible to be pixels of the true NT contour due to the NT contour's property mentioned in the introduction. The basic idea guarantees the extracted contour close. While with the GVF snake, the discontinuousness of the NT contour can be dealt with.

In the algorithm, we assign pixels of class 1 and class 4 the largest cost value. Since pixels in class 1 are surely on the true NT contour while pixels in class 4 are surely not, assigning them the largest cost value prevents the dynamic programming searching along the wrong direction. Because the cost value of class 2 is larger than that of class 4. The close curve in the edge map has the higher priority to be the true NT contour than the curve extracted by the GVF snake. So the algorithm realizes the basic idea of extracting the NT contour. Two key difficulties mentioned in the introduction are well figured out with this proposed scheme.

### 4.2. NT parameters

The NT thickness is one of the most discriminating parameters in the first trimester of pregnancy. However, the NT thickness is not very sensitive [2]. Since the NT is the accumulation of fluid in the fetus nuchal region, the NT area is

more sensitive to the accumulation than the NT thickness. With this proposed scheme, the NT area can be also estimated.

It is noted that with the NT contour many other parameters can be extracted. The effect of these new parameters including the NT area should be testified in the further work.

## 5. CONCLUSION

A novel scheme is proposed to extract the NT contour automatically. After a morphologic filtering, this scheme establishes the edge map and extracts a preliminary contour by the GVF snake. Then an algorithm is presented to compound the edge map and the preliminary contour to obtain the final NT contour based on the dynamic programming. Compared with manual measurements, this automated approach reduces problems of the variability and reproducibility. With the NT contour, NT parameters can be calculated for the clinical use.

## REFERENCES

- [1] M. A. Zoppi, R. M. Ibba, M. Floris, *et al.*, "Changes in nuchal translucency thickness in normal and abnormal karyotype fetuses," *BJOG: an International Journal of Obstetrics and Gynaecology*, Vol. 110, pp. 584–588, June 2003.
- [2] N. Montenegro, A. Matias, J. C. Areas, S. castedo and H. barros, "Increased fetal nuchal translucency: possible involvement of early cardiac failure," *Ultrasound Obstet. Gynecol.*, Vol. 10, pp.265–268, 1997.
- [3] A. P. Souka, E. Krampl, S. Bakalis, V. Heath, and K. H. Nicolaides, "Outcome of pregnancy in chromosomally normal fetuses with increased nuchal translucency in the first trimester," *Ultrasound Obstet. Gynecol.*, Vol. 18, pp.9–17, 2001.
- [4] R. J. Snijders, P. Noble, N. Sebire, A. Souka, K.H. Nicolaides, "UK multicentre project on assessment of risk of trisomy 21 by maternal age and fetal nuchal translucency thickness at 10-14 weeks of gestation," *The Lancet*, Vol. 352, pp.343–346, 1998.
- [5] F. Bernadino, R. Cardoso, N. Montenegro, J. Bernardes, and J. Marques de Sa, "Semiautomated ultrasonographic measurement of fetal nuchal translucency using a computer software tool," *Ultrasound in Med. & Biol.*, Vol. 24, pp.51–54, 1998.
- [6] Z. Tao, and H. D. Tagare, "Tunneling descent for m.a.p. active contours in ultrasound segmentation," *Medical Image Analysis*, Vol.11, pp. 266–281, 2007.
- [7] C. Davatzikos, and J. L. Prince, "An active contour model for mapping the cortex," *IEEE Trans. Med. Imag.*, Vol. 14, pp. 65–80, Mar. 1995.
- [8] A. J. Abrantes and J. S. Marques, "A class of constrained clustering algorithms for object boundary extraction," *IEEE Trans. Image Processing*, Vol. 5, pp. 1507–1521, Nov. 1996.
- [9] C. Xu, and J. L. Prince, "Snakes, Shapes, and Gradient Vector Flow," *IEEE Trans. Image Processing*, Vol. 7, pp. 359–369, Mar. 1998.
- [10] J. Tian, S. L. Bao, and M. Q. Zhou, *Medical image process and analysis*. Publishing house of electronics industry, 2003.
- [11] L. Busse, T. R. Crimmins, and J. R. Fienup, "A model based approach to improve the performance of the geometric filtering speckle reduction algorithm," *Proc. IEEE Ultrason. Symp.*, pp.1353–1356, 1995.
- [12] R. C. Gonzalez, R. E. Woods, *Digital image processing (second edition)*. Pearson Education Inc., 2002.
- [13] T. R. Crimmins, "Geometric Filter for Speckle Reduction," *Applied Optics*, Vol. 24, pp.1438–1443, 1985.
- [14] T. R. Crimmins, "Geometric Filter for Reducing Speckle," *Applied Optics*, Vol. 25, pp. 651–654, 1986.
- [15] Y. Yu, and S. T. Acton, "Speckle Reducing Anisotropic Diffusion," *IEEE Trans. Image Processing*, Vol. 11, pp.1260–1270, Nov. 2003.